

Different acquisition arcs for better imaging left ventricular wall in myocardial perfusion single photon emission tomography

Kemin Huang BS,
Yanlin Feng MD,
Dejun Liu MD,
Wen Li MD,
Weitang Liang BS,
Lin Li BS

Department of Nuclear Medicine,
The First People's Hospital of
Foshan, Foshan 528000,
Guangdong, China.

Keywords: Myocardial perfusion

-SPET imaging
-Left ventricular wall
-Better imaging
-Acquisition arcs

Corresponding author:

Yanlin Feng MD
Department of Nuclear Medicine,
The First People's Hospital of
Foshan, Foshan 528000,
Guangdong, China
hkmin@fsyyy.com

Received:

9 July 2018

Accepted revised:

1 August 2018

Abstract

Objectives: Conventional single-photon emission tomography (SPET) myocardial perfusion imaging (MPI) is performed in the supine position range RAO 45°-LPO 45°, but the effect of other acquisition arcs on imaging quality have not been well described. In this study, we compared the radioactivity over left ventricle walls as measured by different acquisition arcs to identify the best specific applications. **Subjects and Methods:** A total of 125 low-risk coronary heart disease patients underwent technetium-99m methoxy isobutyl isonitrile (^{99m}Tc-MIBI) stress MPI, of which 52 received 360° acquisition with reconstruction using different 180° projections and the remaining 73 received conventional 180° (LPO 45°-RAO 45°) and left-side 180°(POST 180°-ANT 0°) acquisition consecutively. We statistically compared the radioactivity and defect score of each left ventricular wall from different acquisition arcs. **Results:** Myocardial slices reconstructed from POST 180°- ANT 0° yielded highest radioactivity uptake for lateral, inferior and septal walls, LPO 45°-RAO 45° for the anterior wall and LPO 35°-RAO 55° for the apical region. Compared to conventional 180° acquisition, the segments with decreased defect scores were observed in 27.67% using left-side 180° acquisition. The proportion was significantly higher for males (P=0.035) and patients with high body mass index (BMI) (P=0.036). Segments with decreased defect scores were mainly in the inferior, septal and lateral walls and more in males than in females in the inferior wall (P=0.004). **Conclusion:** The different arc of data acquisition could significantly affect the appearance of each wall of the left ventricle, POST 180°-ANT 0° acquisition arc represented a significantly enhanced imaging quality of inferior walls as compared to the conventional acquisition arc LPO 45°-RAO 45° in 180 protocol, especially in males.

Hell J Nucl Med 2018; 21(2): 134-139

Published online: 10 August 2018

Introduction

Myocardial perfusion imaging (MPI) is a well-established diagnostic method for evaluation and risk stratification of coronary artery disease (CAD) [1,2]. However, the count density in myocardial perfusion images is dependent on a number of factors, including imaging geometry (such as the contour used, starting angle, range of orbit), attenuation (breast, diaphragmatic and thoracic wall) and scatter. This frequently results in artifacts of varying severity, such as in the anterior wall of females and in the inferior wall of males [3]. Various attenuation correction methods have been used to reduce the incidence of attenuation artifacts. Such investigations have demonstrated that change the attenuation patterns between the diaphragm and heart in the prone position imaging can decrease the risk of attenuation artifacts in the left ventricular inferior wall [4,6]. Techniques such as imaging in the right lateral position were previously suggested [7-8]. Tonge et al. (2008) [9] proposed that the sitting position could significantly enhance patient comfort and decrease the incidence of attenuation artifacts from the diaphragm in non-obese males. In addition, computed tomography (CT) attenuation correction has been widely applied in recent years to compensate for photon attenuation [10-12].

Previous studies on the arc of MPI acquisition have focused mainly on the merits of 180° versus full 360° acquisition [13-15]. Due to the position of the heart in the left frontal chest cavity, 180° acquisition ranging from RAO 45° to LPO 45° is widely recognized as the optimal acquisition arc [16]. However, variable tissue composition produces different attenuation artifacts in single photon emission tomography (SPET) imaging, and any choice of projection arc will change the attenuation patterns of heart walls. This original study was designed to investigate (i) the impact of acquisition arcs on the appearance of left ventricular walls and (ii) whether there are preferential acquisition arcs for

different individuals or patient subgroups.

Subjects and Methods

Patients

A total of 125 cases (age, 60.3 ± 9.6 years, 69 male and 56 female) underwent technetium-99m methoxy isobutyl isonitrile (^{99m}Tc -MIBI) stress MPI in our department between October 2016 and June 2017 were enrolled. All participants were diagnosed with low-risk coronary heart disease based on clinical manifestations, exercise electrocardiogram and ultrasound examination. Voluntary informed consent was obtained from all study population. This study was approved by our Hospitals Ethics Committee.

Group 1 consisted of 52 cases, 27 male and 25 female, 23 with normal body mass index (BMI) 18.8 - $25\text{kg}/\text{m}^2$ and 29 with high BMI (25.1 - $33.7\text{kg}/\text{m}^2$). The patients received 360° data acquisition. Group 2 consisted of 73 patients, 42 male and 31 female, 39 with normal BMI (18.5 - $25\text{kg}/\text{m}^2$) and 34 with high BMI (25.1 - $32.8\text{kg}/\text{m}^2$). All these patients underwent conventional 180° (LPO 45° -RAO 45°) and left-side 180° (POST 180° -ANT 0°) acquisition.

Full 360° data acquisition protocol

Fifty-two patients (Group 1) underwent the treadmill exercise stress test, and 740MBq of ^{99m}Tc MIBI were injected intravenously (i.v.) at the peak of exercise. Single photon emission tomography examination with a low-energy high-resolution collimator (symbia T16 SPET/CT, Siemens, Germany). Images were acquired throughout a body-contour orbit using two detectors angled at 180° , over a 360° arc starting from the anterior to the posterior position. Acquisition settings were 20% energy window centered at 140 keV, step-and-shoot mode, 72 projections (5° per step), 30 s per projection, 64×64 matrix size, and 1.45 zoom.

The cardiac and extra-cardiac signals were estimated from all projection images by small rectangular regions of interest (ROI) placed over the area with the maximum intestinal tract and maximum myocardial activity (and the) percentage of intestinal-to-myocardial count was calculated. Raw data from the 72 projections were divided into eight areas (9 projections per area), each representing 45° of the acquisition arc (Figure 1). The count density of myocardial and the myocardial/intestinal count ratios at different areas were also compared.

Raw data reconstruction at different arcs

Cinematic displays, sinograms and linograms of emission data were scrutinized for motion. Raw data of consecutive 180° projections starting at different initial angles were selected from the full 360° data set for image reconstruction. Starting from -180° , image reconstruction was performed at an angle interval of 5° from -180° to 0° , -175° to 5° , -170° to 10° , and so on. Images were reconstructed from a total of 37 contiguous 180° arcs. Image reconstruction was performed using the 3-dimensional ordered subset expectation maximization met-

hod employed collimator resolution recovery corrections with 8 subsets, 6 iteration, and 5mm layer thickness. Reconstruction images were reoriented along the short-axis, horizontal long-axis, and vertical long-axis images of the left ventricle.

Bull's eye images (perfusion polar plots) were produced using QPS software (2009 version) and divided into the anterior, lateral, septal, apical, and inferior wall segments. The percentages of maximum radioactivity uptake (average count of each segment in relation to the pixel showing the maximum activity) in each segment of the left ventricle were compared among the reconstruction arcs.

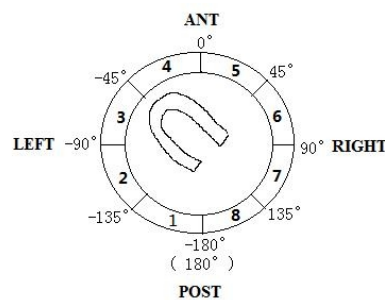


Figure 1. The 360° acquisition data from the 72 projections were divided into eight areas (9 projections per area), each representing 45° of the acquisition arc.

Comparison of 180° data acquisition using two arcs

Seventy-three patients (Group 2) were studied as described above in Group 1. Two consecutive protocols of data acquisition were performed: Protocol 1 with conventional 180° acquisition ranging from LPO 45° to RAO 45° and Protocol 2 with left-side 180° acquisition ranging from POST 180° to ANT 0° . The acquisition sequence was determined randomly. The two detectors were positioned at 90° . Thirty-six projections (5° per step) were acquired at 30s per projection. Other acquisition parameters and reconstruction procedures were as described in Group 1. Images of the myocardial short-axis, horizontal long-axis, and vertical long-axis were reconstructed. The percentages of maximum uptake by each left ventricular wall segment were obtained according to bull's eye images. The difference between conventional 180° and left-side 180° acquisition were statistically analyzed.

The myocardium was divided into 5 segments (anterior, lateral, septal, apical, and inferior wall) and was examined by three experienced nuclear medicine physicians. The physicians did not know about the patients and acquisition arcs. A report on the extent of perfusion defects of all segments were evaluated using a 5 points scoring system: 0 was normal, 1 was mild reduction of radioisotope uptake, 2 was moderate reduction of radioisotope uptake, 3 was severe reduction of radioisotope uptake and 4 absence of detectable tracer uptake. Final outcomes were obtained according to the consensus of two independent physicians. The changes in defect score from conventional 180° to left-side 180° acquisition in all segments were compared.

Statistical analysis

Statistical software SPSS 17.0 was used for data analysis. All

Table 1. The average counts from myocardial and intestinal tract ROI and the ratio of myocardial to intestinal tract in different areas (arcs).

ROI	Area 1	Area 2	Area 3	Area 4	Area 5	Area 6	Area 7	Area 8
Heart	208.97 ±7.57	245.30 ±27.99	309.73 ±12.47	325.15 ±7.93	269.10 ±19.20	202.30 ±9.99	170.97 ±13.96	176.34 ±16.39
Intestinal	605.84 ±65.67	617.47 ±74.99	905.13 ±128.74	1517.85 ±177.20	1906.37 ±35.60	1740.92 ±143.36	1227.45 ±144.58	832.18 ±46.20
Heart/intestinal	0.35 ±0.02	0.40 ±0.02	0.35 ±0.03	0.22 ±0.03	0.14 ±0.01	0.12 ±0.01	0.14 ±0.01	0.21 ±0.03

data are expressed as mean±standard deviation ($\bar{x}\pm SD$). The difference in percentage of maximum uptake between conventional 180° and left-side 180° acquisition protocols was compared by paired t-test. Ratios were compared using chi square test. $P<0.05$ was considered statistically significant.

Results

Variations in the activity of myocardial and intestinal tract from the projection images acquired at different arcs

The activity of myocardial images differed markedly among the different projection images obtained at different arcs (Figure 2). Areas 1-5 (POST 180° to RAO 45°) showed high myocardial activity, while areas 6-8 (RAO 45°-POST 180°) showed low myocardial activity.



Figure 2. Examples of typical projection images appearance, in males with a normal BMI of 23.65, 360° acquisition data from the 72 projections divided into eight areas as described in Figure 1. The a-e (areas 1-5, POST 180° to RAO 45°) showed high myocardial radioactivity, while f-h (areas 6-8, RAO 45°-POST 180°) showed low radioactivity (arrows).

Significant changes were noted in the radioactivity counts from the myocardial and intestinal tract at different projection angles, especially for the intestinal tract (Figure 3), the projection images from -130° to 50° yielded high myocardial

counts and the -80° to 145° yielded high intestinal counts, respectively. The average counts from myocardial and intestinal tract ROI and the ratio of myocardial to intestinal tract in different areas (45 arcs) are presented in Table 1. The myocardial radioactivity counts in areas 3 and 4 were relatively high, with the highest value in area 4. The intestinal tract radioactivity counts from areas 4, 5 and 6 were also relatively high, especially in area 5. The myocardial /intestinal count ratios in areas 1, 2 and 3 were relatively higher compared to the other areas.

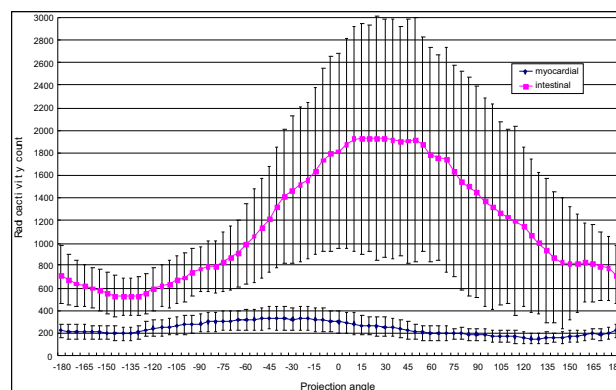


Figure 3. The radioactivity counts from the myocardial and intestinal tract at different projection angles showing significant changes, especially for the intestine.

Effect of raw data reconstruction at different arcs on myocardial SPET

The percentages of maximum radioactivity uptake of each left ventricular wall segment differed significantly depending on the reconstruction arc (Figure 4). The highest radioactivity uptake for each left ventricular wall segment was observed using a reconstruction arc which differed from the conventional arc. The peak radioactivity uptake from the lateral, inferior and septal walls yielded using POST 180°-ANT 0° reconstruction. Highest radioactivity uptake from the anterior wall was obtained using LPO 45°-RAO 45° and that from the apical region using LPO 35°-RAO 55°.

Myocardial image quality also differed significantly depending on the raw data reconstruction arc (Figure 5). High-quality images could be obtained within the range LPO 45°-RAO 45° (areas 2-5) and POST 180°-ANT 0° (areas 1-4). However, some left ventricular wall segments were not fully displayed and showed image distortion in reconstructions within LL 90°-RL 90° (areas 3-6), LAO 45°-RPO 45° (areas 4-7) and ANT 0°-POST 180° (areas 5-8).

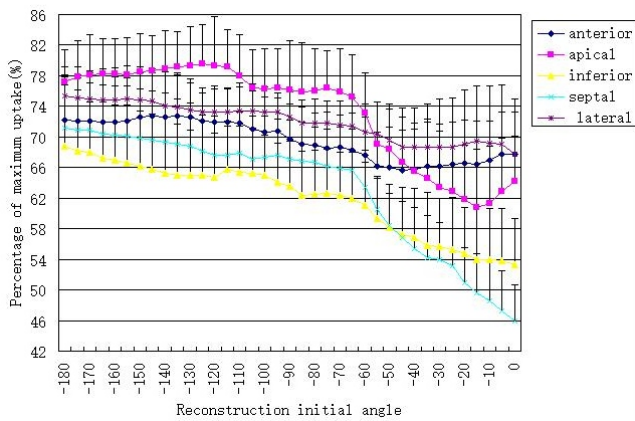


Figure 4. Changes in radioactivity uptake of each left ventricular wall segment at different initial reconstruction angles (different reconstruction arcs). The relationship between the initial reconstruction angle and range of imaging reconstruction: -180° corresponded to the reconstruction range from POST 180° to ANT 0°, -170° from LPO 80° to RAO 10°, -160° from LPO 70° to RAO 20° and so on.

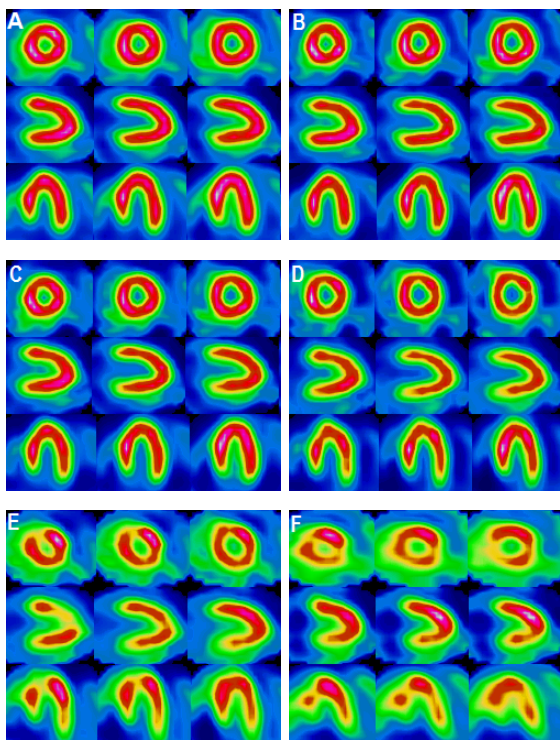


Figure 5. The myocardial SPET image depending on the different reconstruction arcs from a female with normal BMI of 23.73. A: The images reconstructed from areas 1-8 (full 360 projections). B and C: The images reconstructed from areas 1-4 (POST 180°-ANT 0°) and areas 2-5 (LPO 45°-RAO 45°) showed high-quality segments of left ventricular wall. D-F: Images reconstructed from areas 3-6 (LL 90°-RL 90°), are-as 4-7 (LAO 45°-RPO 45°) and areas 5-8 (ANT 0°-POST 180°), some segments are not fully displayed but imaging distortion is apparent.

Comparison of images between conventional 180° and left-side 180° acquisition protocols

The percentages of maximum uptake by each left ventricular wall segment using conventional 180° and left-side 180° acquisition are presented in Table 2. The radioactivity uptake from inferior, septal and lateral walls were significantly lower using conventional 180° acquisition (all P<0.001), whereas

the radioactivity uptake from the anterior wall was considerably higher using conventional acquisition compared to left-side 180° acquisition (P=0.004). The radioactivity uptake from the apical region did not differ significantly between the two acquisition arcs (P=0.319).

Table 2. Comparison of percentage maximum uptake by each left ventricular wall segment using conventional 180° and left-side 180° acquisition (%).

Acquisition	Anterior	Apical	Inferior	Septal	Lateral
Conventional 180° (LPO 45°-RAO 45°)	73.39 ±4.47	77.18 ±6.20	66.99 ±5.64	68.48 ±4.75	72.21 ±4.37
Left-side 180° (POST 180°-ANT 0°)	72.27 ±5.36	76.70 ±5.45	71.01 ±5.66	71.66 ±5.57	73.84 ±4.41
T	2.991	1.003	-11.608	-8.293	-3.834
P	0.004	0.319	<0.001	<0.001	<0.001

Compared to conventional 180° acquisition, the activity distributions from the left ventricular inferior, septal, and lateral walls were improved by varying degrees using left-side 180° acquisition, with the most significant improvement in the inferior walls of male patients (Figure 6). The changes in defect score, from conventional 180° to left-side 180° acquisition, for each left ventricular wall segment and different gender and BMI are presented in Figure 7. Of 365 wall segments from 73 patients, segments with increased defect score were observed in 5.75% (21/365), segments with no change in 66.58% (243/365), and with decreased defect score in 27.67% (101/365). The percentage of wall segments with decreased defect score was higher in males than in females (31.9%, 67/210 vs. 21.93%, 34/155; $\chi^2=4.428$, P=0.035) and in patients with high BMI compared to normal BMI (32.94% (56/170) vs. 23.08% (45/195); $\chi^2=4.415$, P=0.036). The segments with increased defect scores were observed mainly in the anterior wall (10.96%; 8/73) and the apical region (12.33%; 9/73), while segments with decreased defect scores were predominantly in the inferior (54.79%; 40/73), septal (30.13%; 22/73), and lateral walls (34.24%; 25/73). The percentage of patients with decreased defect score over the inferior wall was significantly higher in males than in females (69.04%, 29/42 vs. 35.48%, 11/31; $\chi^2=8.111$, P=0.004), but no statistical difference was observed between subjects with high and normal BMI (55.88%, 19/34 vs. 53.84%, 21/39; $\chi^2=0.030$, P=0.862).

Discussion

Full 360° acquisition is commonly adopted in conventional non-cardiac SPET to gain more information from the target organ. Nevertheless, the angular range of data collection in myocardial SPET is a subject of controversy. Multiple studies

have compared myocardial 180° and 360° acquisition protocols [17-20]. Myocardial 180° SPET can enhance imaging contrast, and shorten the imaging time by the use of single-head or orthogonally positioned dual-head gamma camera systems. Nevertheless, it may cause attenuation artifacts and even image distortion in certain myocardial segments. Full 360° acquisition can enhance image quality, decreased attenuation artifacts, and accurately estimate the defect size, but may exacerbate the influence of intestinal tract activity on myocardial images. In addition, the detector is farther from the heart at certain points, which probably decreases image resolution. In this study, we demonstrate that the activity of myocardial and intestinal tract differed according to the projection images at different arcs (Figure 3). For instance, projection images of areas 6-8 (RAO 45°-POST 180°) with low information of myocardial and with a relatively low ratio of myocardial to intestinal tract radioactivity count. Consequently, the projection images of these areas can not be utilized for information of myocardial perfusion. Instead, these acquisition arcs may negatively affect the image quality due to attenuation and scattering. Therefore, these acquisition arcs should be avoided in clinical SPECT myocardial perfusion imaging.

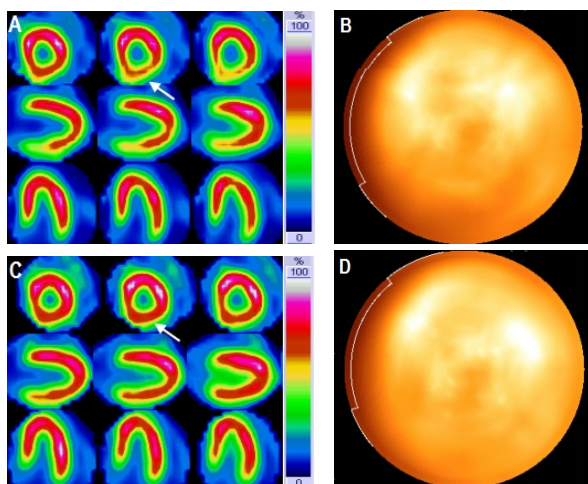


Figure 6. Comparison of the conventional 180° and left-side 180° acquisition images from a male with high BMI of 25.72. A and B: The conventional 180° acquisition images and perfusion polar plots showed low radioactivity in the inferior wall. D and C: The left-side 180° acquisition images and perfusion polar plots showed significantly higher radioactivity (arrows).

For the 180° acquisition protocol, the preferred orbit or angular sample range is 180° from RAO 45° to LPO 45° because of the anterior position of the heart in the left hemithorax. Due to differences in density and radioactivity, the uptake by tissues surrounding the heart, attenuation and scattering for each left ventricular wall segment vary according to the acquisition arc. In our investigation, the raw data from 72 projections were divided into eight regions (Table 1). The cardiac radiation counts in areas 2-5 were relatively high, indicating that these areas are less affected by attenuation. The myocardial/intestinal tract count ratios in areas 1-3 were relatively high, indicating that these regions are less affected by scattering. Moreover, myocardial slices reconstructed from

different arcs yielded the highest radioactivity uptake for each left ventricular wall segment differed significantly depending on the reconstruction arc (Figure 4). The high-quality images could be obtained within the range of LPO 45°-RAO 45° (areas 2-5) and POST 180°-ANT 0° (areas 1-4) (Figure 5). These results suggest that the conventional RAO 45°-LPO 45° range is not the only option for all walls in 180° acquisition protocol. For certain segments, change in acquisition arcs may significantly enhance the radioactivity and improve image quality. In previous studies, 240° acquisition (LPO 15°-RAO 75°) [21] and an overlapping 180 degrees orbits were adopted [22], which successfully improved the image quality and increased sensitivity of myocardial perfusion imaging. In our study, we compared the activity of myocardial from all 360° projection images, and the image quality reconstructed from different areas, indicating that the POST 180°-ANT 0° acquisition arc can better imaging left ventricular wall.

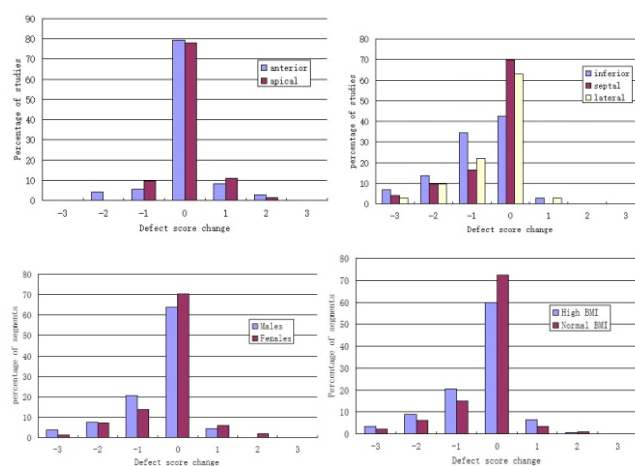


Figure 7. The changes in defect score from conventional 180° to left-side 180° acquisition for each left ventricular wall segment and different gender and BMI. A: Anterior and apical segments. B: Inferior, septal, and lateral segments. C: Males and females. D: High BMI and normal BMI. In the abscissa, the negative numbers represent decreased defect scores, the positive numbers represent increased defect scores and 0 represent no change in the defect scores.

Attenuation and tissue scattering are critical factors influencing the quality of myocardial imaging [23]. In conventional RAO 45°-LPO 45° acquisition, attenuation artifacts in the inferior wall are induced by attenuation from the diaphragm. Given the anatomical relationship between heart and diaphragm, the arc range from RAO 45° to the ANT 0° is most likely affected by the right hemi-diaphragm. However, in the left-side 180° acquisition area (POST 180°-ANT 0°) that the overlap of the heart and diaphragm were reduced and the attenuation patterns of heart were changed. It reduces the photon attenuation of the diaphragm to the heart, thus increase the radioactivity of inferior, septal and lateral wall of the left ventricle. The LPO 45°-POST 180° arc can theoretically increase the attenuation of a homogeneous examination couch. However, myocardial tomography involves relative imaging based on myocardial radioactivity uptake after standardization to the maximal activity. Anyhow, the attenuation from homogeneous medium exerts slight effect on each segment of the left ventricle [24].

Previous studies have demonstrated that high radioactivity uptake by abdominal organs (such as liver or intestinal tract) can affect the quality of myocardial tomography [25-27]. Photon scatter within the myocardium reduces image contrast and scatter from extra-cardiac activity and can interfere with uniformity, especially of the inferior wall. In our study, we compared the radioactive count of the intestinal tract and the myocardial/intestinal tract ratio between areas 1 and 5 (Table 1), found that the radioactivity count of intestinal in the area 5 was significantly higher than that in area 1, and the ratio of heart to intestine was significantly lower than that in area 1, indicating that the influence of the scattering in the area 5 was significantly higher than that in area 1. Because of the POST 180°-ANT 0° acquisition range excludes the angle of the area 5, thus that the effect of scattering is also significantly reduced. As a consequence, the image quality of the inferior wall of the left ventricle is obviously better than that of the conventional RAO 45°-LPO 45° acquisition range that containing area 5 (Figure 6).

The attenuation by tissues surrounding myocardium varies substantially among individuals according to gender and body shape. Consequently, the effect of attenuation artifacts on each left ventricular segment also differs among individuals. Previous studies investigating the differences in CT attenuation correction among individuals according to gender and body shape [9, 10] found that CT attenuation correction possessed significantly higher diagnostic accuracy for male patients with coronary heart disease than for female counterparts, and for obese patients compared with those with normal body weight, as we have also found that the image quality of high BMI patients, especially male subjects, can be significantly improved by using the left side 180° acquisition.

In conclusion, specific segments of the left ventricular wall are best imaged using different SPET-MPI acquisition arcs. Continuous acquisition within the range POST 180°-ANT 0° can significantly enhance radioactivity in the inferior, septal and lateral walls, thereby enhancing image quality and especially of the inferior wall in male patients. Taken together, left side 180° acquisition (POST 180° to ANT 0°) can be used for better MPI studies in clinical practice.

Bibliography

- Karacavus S, Celik A, Tutus A et al. Can left ventricular parameters examined by gated myocardial perfusion scintigraphy and strain echocardiography be prognostic factors for major adverse cardiac events? *Hell J Nucl Med* 2014; 17(1): 10-1.
- Tzonevska A, Tzvetkov K, Dimitrova M, Piperkova E. Assessment of myocardial viability with ^{99m}Tc-sestamibi-gated SPET images in patients undergoing percutaneous transluminal coronary angioplasty. *Hell J Nucl Med* 2005; 8(1): 48-53.
- Singh B, Bateman TM, Case JA, Heller G. Attenuation artifact, attenuation correction, and the future of myocardial perfusion SPECT. *J Nucl Cardiol* 2007; 14: 153-64.
- Takuji K, Nobuhiko O, Yoshio T. Diagnostic accuracy of supine and prone thallium-201 stress myocardial perfusion single-photon emission computed tomography to detect coronary artery disease in inferior wall of left ventricle. *Ann Nucl Med* 2008; 22: 317-21.
- Shin JH, Pokharna HK, Williams KA et al. SPECT myocardial perfusion imaging with prone-only acquisitions: Correlation with coronary angiography. *J Nucl Cardiol* 2009; 16: 590-6.
- Arsanjani R, Hayes SW, Fish M et al. Two-position supine/prone myocardial perfusion SPECT (MPS) imaging improves visual inter-observer correlation and agreement. *J Nucl Cardiol* 2014; 21: 703-11.
- Huang K-M, Feng Y-L, Wen G-H et al. The value of right lateral decubitus position to decrease artificial defect of cardiac anterior wall in ^{99m}Tc-MIBI SPECT myocardial perfusion imaging for women. *Chin J Nucl Med Mol Imaging* 2013; 33: 444-7.
- Heiba SI, Hayat NJ, Salman HS et al. Technetium-99m-MIBI myocardial SPECT: supine versus right lateral imaging and comparison with coronary arteriography. *J Nucl Med* 1997; 38: 1510-4.
- Tonge CM, Armstrong IS, Arumugam P et al. Changes in the appearance of attenuation artefacts due to change in posture in myocardial perfusion imaging. *Nucl Med Commun* 2008; 29: 441-7.
- Huang R, Li F, Zhao Z et al. Hybrid SPECT/CT for attenuation correction of stress myocardial perfusion imaging. *Clin Nucl Med* 2011; 36: 344-9.
- Apostolopoulos DJ, Savvopoulos C. What is the benefit of CT-based attenuation correction in myocardial perfusion SPET? *Hell J Nucl Med* 2016; 19(2): 89-92.
- Sharma P, Patel CD, Karunanithi S et al. Comparative accuracy of CT attenuation-corrected and non-attenuation-corrected SPECT myocardial perfusion imaging. *Clin Nucl Med* 2012; 37: 332-8.
- O'Connor MK, Hruska CB. Effect of tomographic orbit and type of rotation on apparent myocardial activity. *Nucl Med Commun* 2005; 26: 25-30.
- He X, Links JM, Gilland KL et al. Comparison of 180 degrees and 360 degrees acquisition for myocardial perfusion SPECT with compensation for attenuation, detector response, and scatter: Monte Carlo and mathematical observer results. *J Nucl Cardiol* 2006; 13: 345-53.
- Apostolopoulos DJ, Spyridonidis T, Skouras T et al. Comparison between 180° and 360° acquisition arcs with and without correction by CT-based attenuation maps in normal hearts at rest. *Nucl Med Commun* 2008; 29: 110-9.
- Holly TA, Abbott BG, Al-Mallah M et al. Single photon emission computed tomography. ASNC imaging guidelines for nuclear cardiology procedures. *J Nucl Cardiol* 2010; 17: 941-73.
- Chen M, Jaszczak RJ, Bowsher JE, Gilland DR. An evaluation of cardiac uniformity, contrast, and SNR with dual-head 180 degrees and triple-head 360 degrees SPECT scans. *IEEE Trans Nucl Sci* 2001; 48: 1428-34.
- LaCroix KJ, Tsui BMW, Hasegawa BH. A comparison of 180 degrees and 360 degrees acquisition for attenuation-compensated thallium-201 SPECT images. *J Nucl Med* 1998; 39: 562-74.
- Freeman MR, Konstantinou C, Barr A, Greyson ND. Clinical comparison of 180-degree and 360-degree data collection of technetium ^{99m}Tc sestamibi SPECT for detection of coronary artery disease. *J Nucl Cardiol* 1998; 5: 14-8.
- Liu YH, Lam PT, Sinusas AJ, Wackers FJ. Differential effect of 180 degrees and 360 degrees acquisition orbits on the accuracy of SPECT imaging: quantitative evaluation in phantoms. *J Nucl Med* 2002; 43: 1115-24.
- Hamby AS, Dobbeleir A, Stulens E et al. 240 degrees: why not? *Nucl Med Commun* 1996; 17: 583-90.
- Wallis JW. Increased sensitivity through use of overlapping 180 degrees orbits in clinical myocardial perfusion imaging. *Eur J Nucl Med* 1995; 22: 543-7.
- Galt JR, Cullom J, Garcia EV. Attenuation and scatter compensation in myocardial perfusion SPECT. *Semin Nucl Med* 1999; 29: 204-20.
- Timmins R, Ruddy TD, Wells RG. Patient position alters attenuation effects in multipinhole cardiac SPECT. *Med Phys* 2015; 42: 1233-40.
- Grüning T, Jones IW, Heales JC. Efficacy of various SPECT reconstruction algorithms in differentiating bowel uptake from inferior wall uptake in myocardial perfusion scans. *Nucl Med Commun* 2013; 34: 113-6.
- Nuyts J, DuPont P, Van den Maegdenbergh V et al. A study of the liver-heart artifact in emission tomography. *J Nucl Med* 1995; 36: 133-9.
- King MA, Xia W, DeVries DJ et al. A Monte Carlo investigation of artifacts caused by liver uptake in single-photon emission computed tomography perfusion imaging with Tc-99m labeled agents. *J Nucl Cardiol* 1996; 3: 18-29.